Physics of the Solid State, 2025, Vol. 67, No. 2

06,03,16,13

# Non-empirical calculations of properties of $KNbO_3$ and $RbNbO_3$ crystals

© R.A. Evarestov[1], S.S. Novikov[1,2]

[1] St. Petersburg State University,
St. Petersburg, Russia
[2] Grebenschikov Institute of Silicate Chemistry RAS,
St. Petersburg, Russia
E-mail: r.evarestov@spbu.ru

Received February 15, 2025
Revised February 16, 2025
Accepted February 16, 2025

The present study investigates the electronic and mechanical properties of potassium and rubidium niobates forming temperature-dependent lattices in cubic, tetragonal, orthorhombic or rhombohedral crystal systems. The calculations are based on the framework of density functional theory (DFT) using the HSE06 functional. The dispersion curves for these perovskites were obtained, and it was found that in all phases except rhombohedral $KNbO_3$ has imaginary modes, indicating the instability of the structures. However, for $RbNbO_3$ such a picture was not observed, and except for the phase with cubic unit cell imaginary frequencies in the dispersion dependences were absent. The electronic bands, high-frequency dielectric permittivity, and lattice formation energy, along with other relevant properties, have been calculated for all phases of both $RbNbO_3$ and $KNbO_3$ crystals.

**Keywords:** Rubidium niobate, potassium niobate, phase transitions, electronic and mechanical properties.

DOI: 10.61011/PSS.2025.02.60674.32-25

## 1. Introduction

Perovskite type crystals such as $BaTiO_3$ are widely known as ferroelectrics. These compounds were widely investigated in the 1960s and 1970s. Ferroelectric transitions related to crystalline structural (phase) transitions are a typical feature of these materials. Analysis of symmetry variation in phase transitions in crystals is generally used to solve one of two problems [1]. The first problem is in predicting possible symmetry groups of low-temperature phases when the symmetry of a high-temperature phase is known. The first problem is generally referred to as the Landau problem. The inverse Landau problem — is the prediction of higher symmetry phases with respect to the chosen lower symmetry phase.

This study investigates phase transitions and properties of perovskite structures of potassium niobate ($KNbO_3$) and rubidium niobate ($RbNbO_3$) classified to the $ABO_3$ family ($A = K, Ta, \ldots,\ B = Ba, Nb, \ldots$). Note that the $KNbO_3$ and $RbNbO_3$ crystals are isostructural with the $BaTiO_3$ crystals and have the same sequence of phase transitions [2].

In the $KNbO_3$ case, four phases were observed experimentally: cubic (Pm-3m, SG 221), tetragonal (P4mm SG 99), orthorhombic (Amm2, SG 38) and rhombohedral (R3m, SG160) [3]. All these phases are shown in Figure 1. The experiment for $KNbO_3$ found three successive temperature-reversible phase transitions (cubic-tetragonal-orthorhombic-rhombohedral). However, the specified transitions run with hysteresis, which indicates that these are first-order phase transitions. Moreover, though the space groups of all phases are subgroups of the cubic phase group, their space groups in the tetragonal-orthorhombic sequence are not linked by the group−subgroup relation. For $RbNbO_3$, the phase transition picture changes significantly and there is no general consensus in the literature concerning the stability of the most low-temperature phase. In particular, some authors claim that the rhombohedral phase shall be stable at zero temperature [4], while other authors argue that another crystal lattice might be more stable [5,6].

## 2. Calculation procedure

Computational description of crystalline phases required high computational accuracy of phonon frequencies because they are defined by the second numerical derivatives of full energy with respect to atomic displacements. Therefore, direct-lattice summation requires a high order of accounting for single-electron, Coulomb and exchange integrals. This aspect was considered when selecting calculation details.

This work used the HSE06 hybrid exchange-correlation functional [7] implemented in CRYSTAL17 software [8]. This software is intended for periodic system simulation where localized atomic Gaussian functions are used for approximation of the Bloch crystal orbitals. Comparison of our calculations including five various density functionals (PBE, PBE0, B3LYP, HSESOL, HSE06) with the experimental data for the rhombohedral $KNbO_3$ phase shows the priority of the HSE06 hybrid density functional for correct determination of structure and energy gap

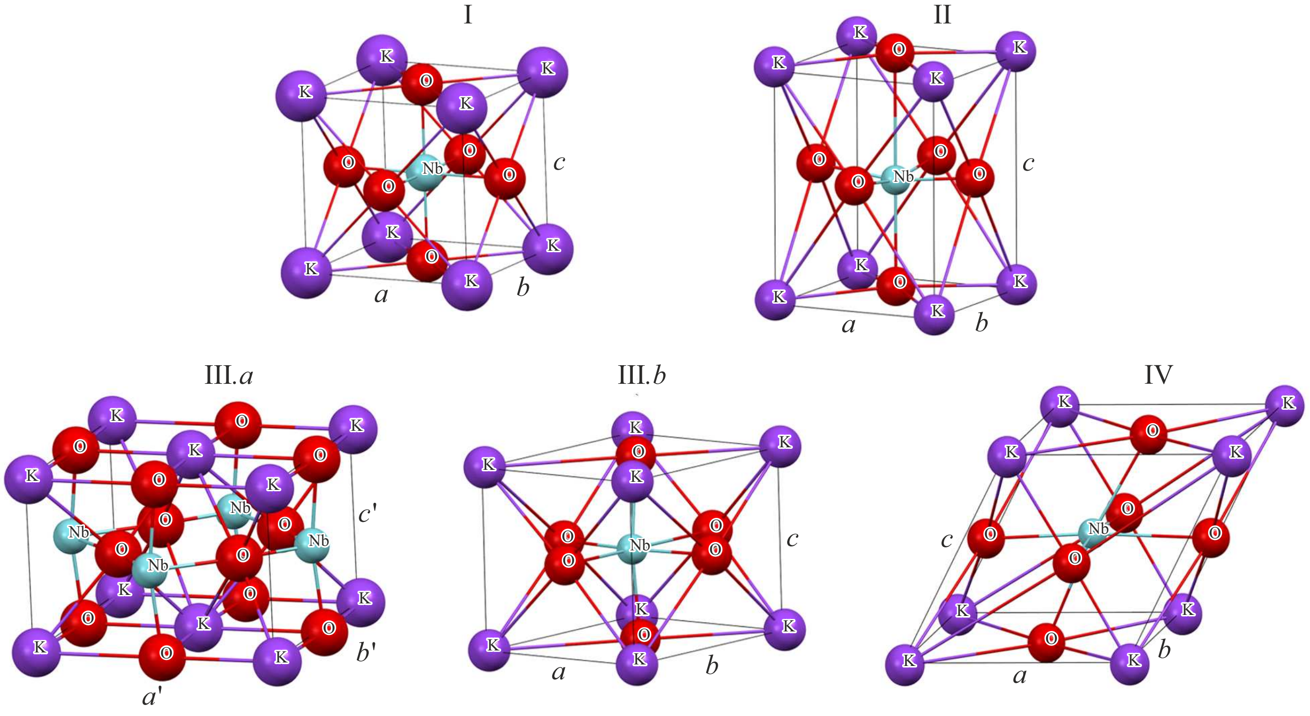

**Figure 1.** Various $KNbO_3$ and $RbNbO_3$ phases: (I) Pm-3m, cubic, (II) $P4mm$, tetragonal, (III) Amm2, orthorhombic (*a*: common orthorhombic lattice cell, *b*: primitive rhombic lattice cell), and (IV) R3m, rhombohedral.

of $KNbO_3$. This conclusion agrees with the findings of [9], where the $KNbO_3$ HSE electronic structure was calculated after comparison of data acquired for five DFT functionals (LDA, PBE, PBEsol, AM05, RTPSS). Sets of atomic bases were taken from CRYSTAL website [8,10]. Sets of DZVP electronic bases were used for K and O atoms [11]. A relativistic pseudopotential and corresponding sets of TZVP bases for valence electrons were used for the Nb atom [12].

The Monkhorst–Pack grid [13] with $8 \times 8 \times 8$ $k$-points and accuracies 8, 8, 8, 8, 16 for single-electron, Coulomb and exchange integrals was used for summation over the Brillouin zone (BZ). Briefly speaking, these values indicate that, during direct-lattice summation, single-electron integrals and two-electron Coulomb integrals lower than $10^{-8}$ are estimated using a multipole expansion, and the two-electron exchange integrals lower than $10^{-16}$ are ignored. The DFT-D2 approximation was used for dispersion correction required to reproduce the Van der Waals interactions [14]. In solving single-electron equations, self-consistency in energy was achieved with accuracy of $3 \cdot 10^{-9}$ eV. Geometry of all studied systems was fully optimized until forces on atoms were not higher than 0.003 eV/Å.

Phonon frequencies were calculated using the following procedure (see the use of this procedure for phonon frequency calculations [15] in four $BaTiO_3$ phases). Equilibrium geometry was first found. A lattice parameter that completely defines the structure was optimized in the cubic phase. Lattice parameters and fractional atomic displacements were optimized in the ferroelectric phases. Atomic and cellular relaxations were performed with an atom force convergence criterion set to 0.005 eV/Å. Energy variation threshold between the optimization steps for self-consistency cycles was $10^{-8}$ eV for structure optimization and $10^{-10}$ eV for phonon frequency calculations.

## 3. *Ab initio* calculations of electronic properties $KNbO_3$ and $RbNbO_3$

Crystalline structures of all above-mentioned four $RbNbO_3$ and $KNbO_3$ perovskite phases were determined experimentally, the corresponding data is available in the Inorganic Crystal Structure Database (ICSD). The latest publications concerning the structure are listed in Table 1 (in brackets). For the orthorhombic Amm2 phase and rhombohedral R3m phase, the structure data is given for the primitive lattice cell (this setting differs from the common setting). Table 1 also compares our calculated structure and band gap data with the data from [9] for $KNbO_3$ (marked with*). These data was obtained using the DFT plane-wave implementation in VASP [16]. The HSE non-local hybrid functional with the Hartree–Fock exact exchange percentage of 30% was used (our HSE06 calculations used 25%). Electron wave functions were extended to cover the kinetic energy of 600 eV. For the rubidium equivalent, the calculated literature data concerning the band gap [4] are also provided (marked with**), where ABINIT with

**Table 1.** Atomic structure and band gap data calculated using the HSE06 functional. Lattice parameters are given in Å. Experimental data is given in brackets and taken from Inorganic Crystal Structure Database (ICSD)

| Space group | Lattice parameters | $RbNbO_3$ | $KNbO_3$ |
|---|---|---|---|
| SG 221 | Lattice parameters | | |
| | $a$, Å | 4.025 (4.025) | 3.983 (4.025) |
| | $b$, Å | 4.025 (4.025) | 3.983 (4.025) |
| | $c$, Å | 4.025 (4.025) | 3.983 (4.025) |
| | $\alpha$, ° | 90° | 90° |
| | $\beta$, ° | 90° | 90° |
| | $\gamma$, ° | 90° | 90° |
| | Atomization energy, eV | 28.872 | 30.611 |
| | Dielectric permittivity | 5.202 | 4.89 |
| | Born effective charges | 1.112 | 1.059 |
| | Rb(K) | 9.269 | 9.177 |
| | Nb | −3.461 | −3.412 |
| | $O_1$ | −3.461 | −3.412 |
| | $O_2$ | −3.461 | −3.412 |
| | $O_3$ | | |
| | Band gap, eV | 2.73, 2.37$^{**}$ | 2.82, 3.14$^{*}$ |
| SG 99 | Lattice parameters | | |
| | $a$, Å | 3.852 (3.997) | 3.967 (3.996) |
| | $b$, Å | 3.852 (3.997) | 3.967 (3.996) |
| | $c$, Å | 5.275 (4.064) | 4.066 (4.063) |
| | $\alpha$, ° | 90° | 90° |
| | $\beta$, ° | 90° | 90° |
| | $\gamma$, ° | 90° | 90° |
| | Atomization energy, eV | 29.066 | 30.638 |
| | Dielectric permittivity | 3.814, 2.828 | 4.673, 4.015 |
| | Born effective charges | 1.236 | 1.084 |
| | Rb(K) | 6.271 | 8.185 |
| | Nb | −1.630 | −2.756 |
| | $O_1$ | −2.938 | −3.256 |
| | $O_2$ | −2.938 | −3.256 |
| | $O_3$ | | |
| | Band gap, eV | 2.88, 2.58$^{**}$ | 2.88, 3.23$^{*}$ |
| SG 38 | Lattice parameters | | |
| | $a$, Å | 3.966 (3.974) | 3.961 (3.971) |
| | $b$, Å | 4.141 (4.037) | 4.024 (4.034) |
| | $c$, Å | 4.141 (4.037) | 4.024 (4.034) |
| | $\alpha$, ° | 89.63° (89.73) | 89.84° (89.72) |
| | $\beta$, ° | 90° | 90° |
| | $\gamma$, ° | 90° | 90° |
| | Atomization energy, eV | 29.014 | 30.643 |
| | Dielectric permittivity | 4.536, 4.144, 3.733 | 4.612, 4.334, 4.066 |
| | Born effective charges | 1.170 | 0.656 |
| | Rb(K) | 4.976 | 5.316 |
| | Nb | −3.069 | −2.764 |
| | $O_1$ | −1.538 | −1.604 |
| | $O_2$ | −1.538 | −1.604 |
| | $O_3$ | | |
| | Band gap, eV | 3.31, 3.25$^{**}$ | 3.30, 3.59$^{*}$ |

**Table 1** (*contd.*)

| Space group | Lattice parameters | $RbNbO_3$ | $KNbO_3$ |
|---|---|---|---|
| SG 160 | Lattice parameters | | |
| | $a$, Å | 4.072 (4.013) | 4.003 (4.013) |
| | $b$, Å | 4.072 (4.013) | 4.003 (4.013) |
| | $c$, Å | 4.072 (4.013) | 4.003 (4.013) |
| | $\alpha$, ° | 89.82° (89.82) | 89.90° (89.82) |
| | $\beta$, ° | 89.82° (89.82) | 89.90° (89.82) |
| | $\gamma$, ° | 89.82° (89.82) | 89.90° (89.82) |
| | Atomization energy, eV | 29.001 | 30.645 |
| | Dielectric permittivity | 4.349, 3.874 | 4.420, 4.108 |
| | Born effective charges | 1.147 | 1.099 |
| | Rb(K) | 7.101 | 7.846 |
| | Nb | −2.749 | −2.982 |
| | $O_1$ | −2.749 | −2.982 |
| | $O_2$ | −2.749 | −2.982 |
| | $O_3$ | | |
| | Band gap, eV | 3.96, 3.57** | 3.53, 3.80* |

**Table 2.** Dependence of the volume compression modulus on the lattice cell symmetry

| Space group | $RbNbO_3$ | $KNbO_3$ |
|---|---|---|
| **SG 221** | 203.94 (GPa) | 215.33 (GPa) |
| **SG 99** | 34.06 (GPa) | 137.89 (GPa) |
| **SG 38** | 32.11 (GPa) | 138.69 (GPa) |
| **SG 160** | 104.20 (GPa) | 142.63 (GPa) |

the GW approximation was used for calculation. Table 1 demonstrates good agreement of our calculated data with the HSE data [9] for $KNbO_3$ and GW data for $RbNbO_3$ [4], and with the experimental structural data.

In case of $KNbO_3$, it is shown that the calculated lattice formation energy decreases in a correct order as the structure stability decreases (with increasing phase existence temperature), while the band gap increases during transition from the high-temperature cubic phase to low-temperature rhombohedral cell, which also agrees with theoretical concepts of the dependence between a band gap and temperature. However, in case of $RbNbO_3$, the dependence is not so unambiguous any longer, and as the band gap increases, the lattice formation energy decreases in the orthorhombic–tetragonal–rhombohedral–cubic lattice sequence. Note also the differences in dielectric constant behavior ($\varepsilon$) as the lattice symmetry varies. Thus, in case of potassium perovskite, the dielectric constant decreases monotonously, while for $RbNbO_3$ $\varepsilon$ takes the minimum value in the orthorhombic lattice. This fact may indicate that the lowest-temperature phase for rubidium niobate has an orthorhombic symmetry.

Electron bands shown in Figure 2 and Figure 3 demonstrate that indirect electronic transition from the valence band to conduction band is inherent in both perovskites in all phases, which agrees with other electronic structure calculation data. The band gap is also in agreement with the literature data [17–21].

## 4. Calculations of phonon and mechanical properties

Phonon frequencies were obtained by the frozen phonon method [22,23] in harmonic approximation with optimized equilibrium crystalline structure parameters. Phonon frequencies in the center of the Brillouin zone (dynamic matrix eigenvalues) are determined from numerical second-order derivative of energy with respect to ground state displacements. For this, the total energy is calculated as found for each crystalline phase of the optimized structure. To obtain phonon frequencies at non-zero wave vectors, a supercell approach is used. Convergence of phonon frequencies and dispersion curves depending on the supercell size was studied by means of *ab initio* frozen phonon calculations.

Figure 4 shows dispersion curves of phonon for various $KNbO_3$ phases. It is shown that imaginary phonon frequencies disappear only for the rhombohedral phase (SG160). This supports the experimental data concerning the stability of this phase at low temperatures. In case of $RbNbO_3$, one dispersion dependence differs (Figure 5) and none of the reviewed phases, except the cubic one, have imaginary frequencies. This fact may suggest that

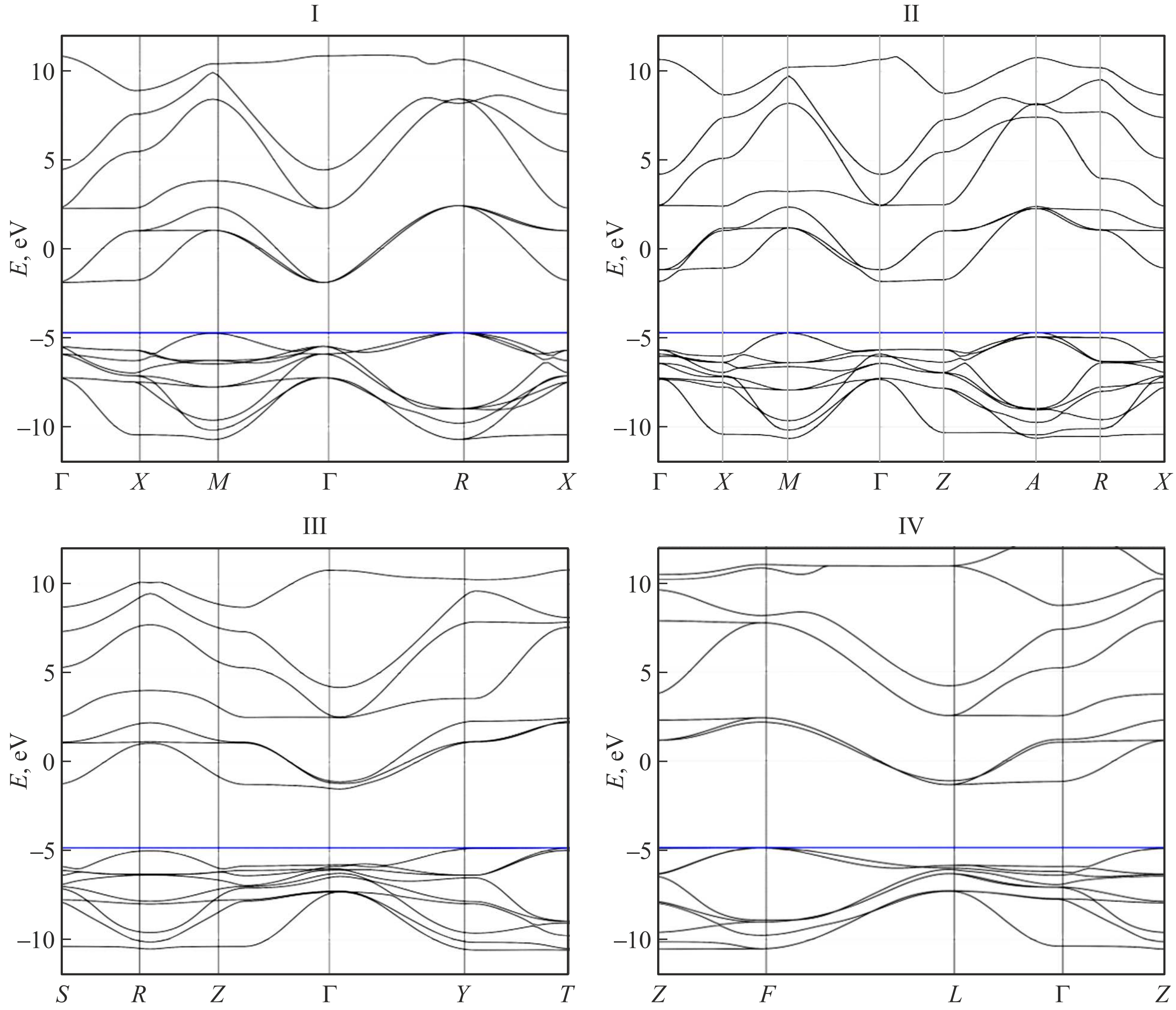

**Figure 2.** Electron bands for various $KNbO_3$ phases: I — cubic phase (SG221); II — tetragonal phase (SG 99); III — orthorhombic phase (SG 38); IV — rhombohedral phase (SG 160).

the corresponding phase transitions that connect the orthorhombic, tetragonal and rhombohedral phases might be the first-order phase transitions. As for the dependence of compression modulus on lattice symmetry (Table 2), note that this dependence for both crystals in non-monotonous and decreases during transition from cubic to orthorhombic lattice, after which increases again during transition to rhombohedral phase.

## 5. Conclusions and findings

*Ab initio* DFT-HSE06 LCAO calculations were performed with optimization of lattice parameters and atomic coordinates for all experimentally observed $KNbO_3$ and $RbNbO_3$ phases. For electronic and structural properties, good agreement with experimental data and DFT plane-wave calculations was found.

A temperature-reversible phase transition sequence was observed for $KNbO_3$. *Ab initio* DFT-HSE06 LCAO calculations of phonon dispersion curves correspond to 0 K. They proved that a stable phase existed only for the lowest-temperature rhombohedral structure. Imaginary frequencies appear for other three phases (see Figure 4), which means that these phases are instable for 0 K. However, calculation data for rubidium perovskite doesn't indicate instability of any phase, except the cubic one, moreover, according to the lattice formation energy calculations, a lattice with orthorhombic crystal system provides the highest energy benefit compared with isolated atoms, whereas the lowest dielectric constant is observed in the same phase.

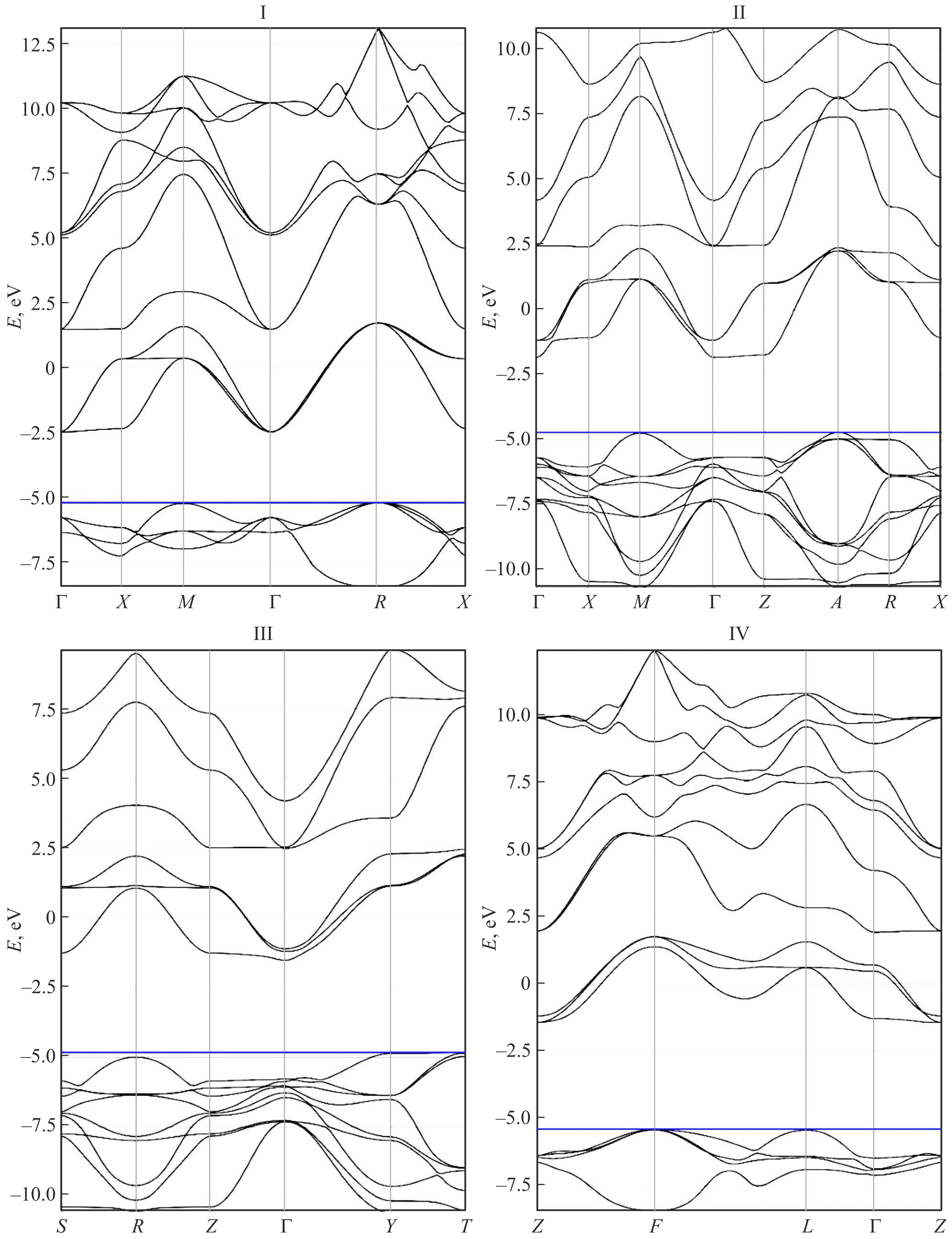

**Figure 3.** Electron bands for various $RbNbO_3$ phases: I — cubic phase (SG221); II — tetragonal phase (SG 99); III — orthorhombic phase (SG 38); IV — rhombohedral phase (SG 160).

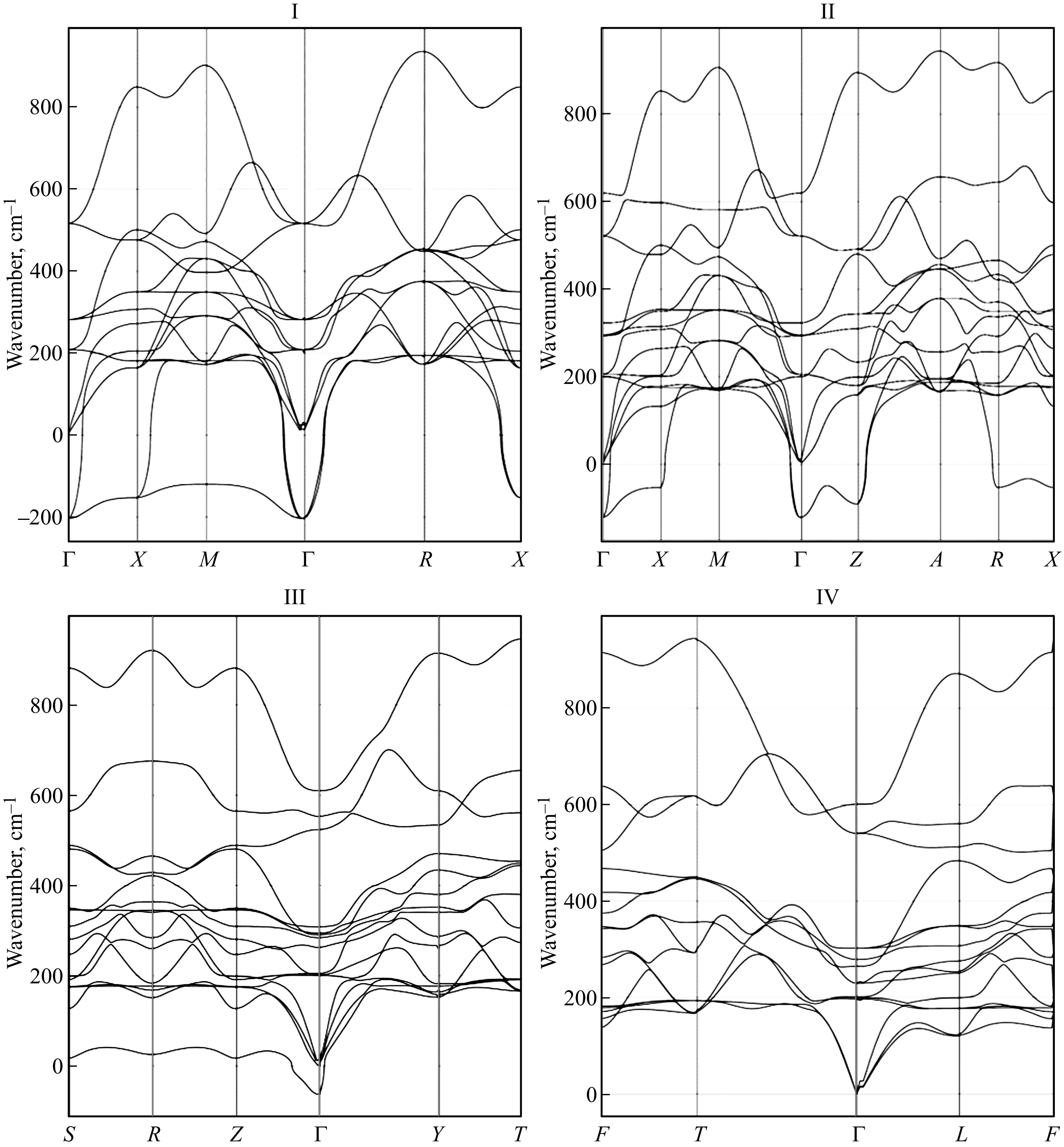

**Figure 4.** Phonon dispersion for various $KNbO_3$ phases: I — cubic phase (SG221); II — tetragonal phase (SG 99); III — orthorhombic phase (SG 38); IV — rhombohedral phase (SG 160).

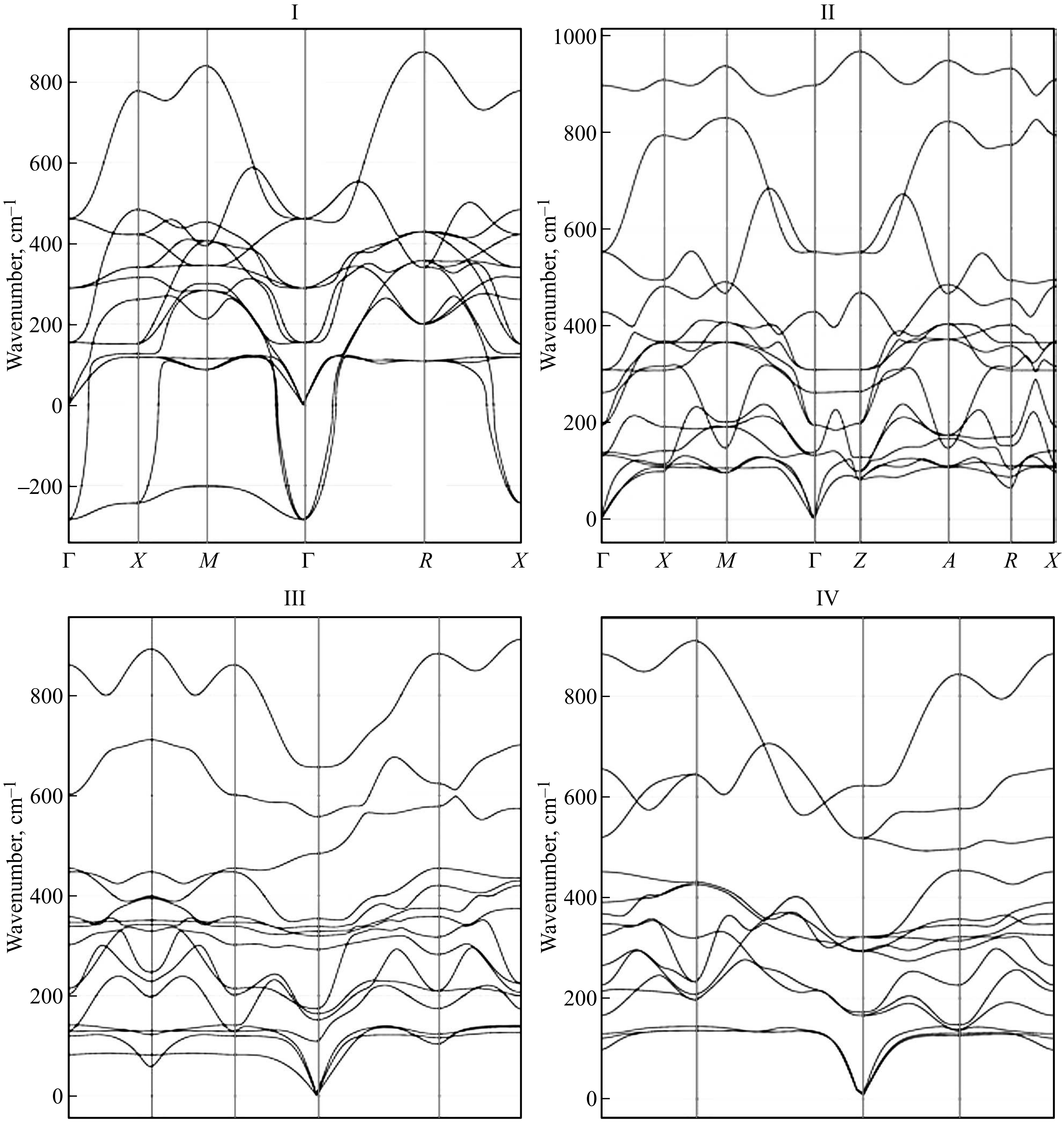

**Figure 5.** Phonon dispersion for various $RbNbO_3$ phases: I — cubic phase (SG221); II — tetragonal phase (SG 99); III — orthorhombic phase (SG 38); IV — rhombohedral phase (SG 160).

### Conflict of interest

The authors declare that they have no conflict of interest.

## References

[1] M. Damnjanović. Eur. J. Phys. **8**, 1 (1987).
[2] R.A. Evarestov. Phys. Rev. B **83**, 134108 (2011).
[3] S.L. Skjærvø, K. Høydalsvik, A.B. Blichfeld, M.-A. Einarsrud, T.R. Grande. Soc. Open. Sci. **5**, 180368 (2018).
[4] A.I. Lebedev. Phys. Solid State **57**, 331 (2015).
[5] A. Yamamoto, K. Murase, T. Sato, K. Sugiyama, T. Kawamata, Y. Inaguma, J.I. Yamaura, K. Shitara, R. Yokoi, H. Moriwake. Dalton Trans. **53**, 7044 (2024).
[6] M. Fukuda, K. Yamaura. J. Ceram.Soc. Jpn **131**, 126 (2023).
[7] J. Heyd, G.E. Scuseria, M. Ernzerhof. J. Chem. Phys. **118**, 8207 (2003).
[8] R. Dovesi, A. Erba, R. Orlando, C.M. Zicovich-Wilson, B. Civalleri, L. Maschio, M. Rérat, S. Casassa, J. Baima, S. Salustro, B. Kirtman. Comput. Mol. Sci. **8**, 1360 (2018).
[9] F. Schmidt, M. Landmann, E. Rauls, N. Argiolas, S. Sanna, W.G. Schmidt, A. Schindlmayr. Adv. Mater. Sci. Eng. **398**, 1317 (2017).
[10] A. Dovesi, V.R.Saunders, C. Roetti, R. Orlando, C.M. Zicovich-Wilson, F. Pascale, B. Civalleri, K. Doll, N.M. Harrison, I.J. Bush, P. D'Arco, M. Llunell, M. Causá, Y. Noël, L. Maschio, A. Erba, M. Rerat, S. Casassa, CRYSTAL17 User's Manual, University of Turin, Torino, Italy (2018).
[11] D.V. Oliveira, M.F. Peintinger, J. Laun, T. Bredow. J. Comput. Chem. **40**, 2364 (2019).
[12] J. Laun, T. Bredow. J. Comput. Chem. **43**, 839 (2022).
[13] H.J. Monkhorst, J.D. Pack. Phys. Rev. B **13**, 5188 (1976).
[14] S. Grimme. J. Comput. Chem. **27**, 1787 (2006).
[15] R.A. Evarestov, A.V. Bandura. J. Comput. Chem. **33**, 1123 (2012).
[16] G. Kresse, J. Furthmuller. Comput. Mater. Sci. **6**, 15 (1996).
[17] S. Simsek, H. Koc, V.A. Trepakov, A.M. Mamedov, E. Ozbay. Ferroelectrics, **461**, 99 (2014).
[18] C.M.I. Okoye, J. Phys. Condens. Matter **15**, 5945 (2003).
[19] M.A. Faridi, S. Tariq, M.I. Jamil, A. Batool, S. Nadeem, A. Amin. Chin. J. Phys. **56**, 1481 (2018).
[20] F.M. Michel-calendini, L. Castet. Ferroelectrics **13**, 367 (1976).
[21] S. Azam, M. Irfan, Z. Abbas, M. Rani, T. Saleem, D.A. Younus, N. Akhtar, B. Liaqat, M. Shabbir, H. Abdullah, G. Al-Sehemi. Dig. J. Nanomater. Biostructures **14**, 751 (2019).
[22] K. Parlinski, Z.Q. Li, Y. Kawazoe. Phys. Rev. Lett. **78**, 4063 (1997).
[23] R.A. Evarestov, M.V. Losev. J. Comput. Chem. **30**, 2645 (2009).

*Translated by E.Ilinskaya*